Experimental Investigation of Concrete with Silica Fume and Hybrid Aspect Ratio Steel Fibers

Mr. Sandeep Gaikwad[1], Mr. Natish Sayyed[2], Mr. Mohitsingh Katoch[3]
[1]Associate Professor, Civil Engineering Department
Tulsiramji Gaikwad Patil College of Engineering and Technology, Nagpur
Email: deepta21@rediffmail.com
[2]Assistant Professor, Civil Engineering Department
Tulsiramji Gaikwad Patil College of Engineering and Technology, Nagpur
Email: profnatishsayyed@gmail.com
[3]Assistant Professor, Civil Engineering Department
Tulsiramji Gaikwad Patil College of Engineering and Technology, Nagpur
Email: mohitkatoch31@gmail.com

Abstract: Adding fibres to concrete greatly increases the toughness of the material. The use of fibres also alters the behaviour of the fibre matrix composite after it has cracked, thereby improving its toughness Secondary cementing materials like Reactive Powder can be used to partially replace cement because of pozzolanic nature. Materials like quartz powder best suites to sand due to its physical and chemical properties, fineness etc. Also these materials are known to increase durability, resistance to sulphate attack. Our main aim is study the materials Quartz powder, Silica Fume are best suitable for preparing durability of concrete for M40 Grade. In cement replaced by silica fume and quartz powder with various percentages like 10%, 15% and 20%. And additional strength purpose using crimped steel fibres and banana fibre with various percentages like 0%, 0.5%, 1%, and 1.5%. This study investigates mechanical properties like compressive strength, Split tensile strength, flexural strength and Durability properties like Acid attack test, Sulphate attack test and Alkalinity attack test and the comparative study of normal concrete and fibres concrete. Now a days, many investigations and experiments are currently going on to prepare a high strengthed and durable concrete by the addition of different types of materials. This research represents the influence of silica fume and steel fibers on normal concrete and will also help in achieving the outstanding results. Hence in this research, Experimental investigations and analysis of results were conducted to study the compressive and flexural behavior of composite concrete with varying percentage of such silica fume and steel fibers added to it. The concrete mix adopted were M40 with varying percentage of the silica fume ranging from 0%, 5%, 10%, 15% & 20% in the partial replacement of cement weight and stainless steel fibers of diameter and length 0.50 mm and 40 mm respectively with the aspect ratio 80 at various percentages ranging from 0%, 0.4%, 1.4%, 2.4% & 3.4% by weight of the concrete. On the analysis of the test results the normal concrete with silica fume and straight steel fibers has enhanced the performance of composite mixture as compared to the ordinary concrete with conventional silica fume and steel fibers which were easily available in the market. These sustainable improvements or modifications could be easily adopted in the regular constructions.

Keywords: Steel fibre, Banana fibre, Silica fume, Quartz powder..

1. Introduction

Concrete is the most widely used construction material in the world due to its excellent compressive strength, durability, and versatility. However, conventional concrete possesses relatively low tensile strength, limited ductility, and poor resistance to crack propagation, making it susceptible to brittle failure under tensile and impact loading. These limitations have encouraged researchers to develop high-performance concrete by incorporating supplementary cementitious materials and fiber reinforcements that enhance both the mechanical and durability characteristics of concrete.

Silica fume, an ultrafine by-product obtained during the production of silicon and ferrosilicon alloys, has emerged as one of the most effective supplementary cementitious materials. Owing to its extremely fine particle size and high silicon dioxide (SiO_2) content, silica fume significantly improves the microstructure of concrete through pozzolanic reactions and filler effects. The addition of silica fume results in increased compressive strength, reduced permeability, enhanced resistance to chemical attack, and improved long-term durability. Nevertheless, the incorporation of silica fume alone may increase the brittleness of concrete because of its dense and rigid matrix.

To overcome this limitation, steel fibers are commonly incorporated into concrete to improve its post-cracking behavior and energy absorption capacity. Steel fibers effectively bridge micro- and macro-cracks, thereby enhancing tensile strength, flexural strength, impact resistance, toughness, and ductility. The performance of fiber-reinforced concrete largely depends on the geometry, length, diameter, volume fraction, and aspect ratio of the fibers. Fibers with different aspect ratios contribute differently to crack control, bond characteristics, and load-carrying capacity.

Hybrid steel fiber reinforcement, involving the combination of steel fibers with different aspect ratios, has gained considerable attention in recent years. Short fibers with lower aspect ratios are effective in controlling the initiation and propagation of micro-cracks, while longer fibers with higher aspect ratios improve resistance to macro-crack development and enhance post-cracking performance. The synergistic action of hybrid aspect ratio steel fibers offers superior mechanical performance compared to the use of a single type of fiber. When combined with silica fume, the dense cementitious matrix provides improved bonding between the steel fibers and the surrounding concrete, resulting in enhanced strength and durability.

Despite significant research on silica fume concrete and steel fiber reinforced concrete individually, limited studies have comprehensively investigated the combined influence of silica fume and hybrid aspect ratio steel fibers on the mechanical properties of concrete. Understanding this combined effect is essential for developing sustainable, high-strength, and durable concrete suitable for modern infrastructure applications such as bridges, industrial floors, pavements, tunnels, high-rise buildings, and earthquake-resistant structures.

Therefore, the present study aims to experimentally investigate the performance of concrete incorporating silica fume and hybrid aspect ratio steel fibers. The research evaluates the influence of varying silica fume replacement levels and combinations of steel fibers with different aspect ratios on the fresh and hardened properties of concrete. The experimental investigation includes workability, compressive strength, split tensile strength, flexural strength, and durability-related characteristics. The findings of this study are expected to contribute to the development of high-performance fiber-reinforced concrete with improved structural efficiency, durability, and service life while promoting the effective utilization of industrial by-products in sustainable construction. Concrete remains the most widely utilized construction material globally, prized for its high compressive strength, versatility, and cost-effectiveness. However, conventional concrete suffers from inherent mechanical limitations, notably low tensile strength, limited strain capacity, and susceptibility to rapid crack propagation under stress. To overcome these deficiencies, modern concrete technology increasingly relies on supplementary cementitious materials (SCMs) alongside fiber reinforcement to engineer high-performance composites capable of enduring severe structural demands.

Among available SCMs, silica fume—an ultra-fine pozzolanic byproduct of silicon and ferrosilicon alloy production—serves a dual physical and chemical role in matrix modification. Chemically, its high amorphous silicon dioxide content reacts with liberated calcium hydroxide Ca(OH)2 during cement hydration to form secondary calcium silicate hydrate (C-S-H) gel, significantly boosting compressive strength. Physically, its sub-micron particles fill micro-voids, refining the pore network and strengthening the fragile interfacial transition zone (ITZ) between aggregate particles and the cement paste.

While silica fume substantially increases compressive strength and matrix density, it simultaneously increases matrix brittleness. Incorporating steel fibers counteracts this brittleness by arresting cracks, imparting post-cracking ductility, and enhancing energy absorption capacity. Rather than relying on a uniform fiber geometry, deploying a hybrid aspect ratio (L/d) strategy optimizes crack control across multiple loading regimes. Short fibers with high aspect ratios bridge micro-cracks during initial loading stages, whereas longer fibers with varying aspect ratios pull across macroscopic cracks during advanced deformation phases.

The primary rationale for this approach lies in the synergistic relationship between matrix densification and multi-scale mechanical bridging: silica fume yields an ultra-dense matrix that enhances fiber-matrix bond strength, preventing premature fiber pull-out and maximizing the efficiency of the hybrid steel fiber network. Despite growing interest in fiber-reinforced concrete, the coupled performance of silica fume densification and hybrid aspect ratio steel fibers requires further empirical evaluation. This study experimentally investigates the mechanical properties, flexural toughness, and structural behavior of concrete engineered with varying silica fume replacement levels alongside targeted combinations of hybrid aspect ratio steel fibers.

2. Literature Review

References

- Adili, E. (2021). Fiber interfacial transition zone concept for steel fiber-reinforced concrete by SEM observation. Journal, Volume(Issue), pages. Cited by: 9

- Deng, Y., Zhang, Z., Shi, C., Wu, Z., & Zhang, C. (2020). Steel Fiber–Matrix Interfacial Bond in Ultra-High Performance Concrete: A Review. Engineering, 22, 215–232. https://doi.org/10.1016/j.eng.2021.11.019 Cited by: 201

Existing research on concrete modified with pozzolanic materials and hybrid fiber reinforcements centers on specific performance parameters:

1. Workability and Fresh State Behavior

- Silica Fume Effect: Due to its ultra-high specific surface area, silica fume increases water demand, leading to a drastic slump loss if uncompensated. Researchers consistently highlight the necessity of polycarboxylate ether (PCE)-based superplasticizers to maintain fluid consistency.
- Fiber Hindrance: Adding high-aspect-ratio steel fibers introduces physical interlocking, which increases internal friction. Studies show that combining macro- and micro-fibers reduces flowability more than mono-fiber mixes, requiring targeted dosage optimization to prevent fiber balling.

2. Microstructural Optimization and Interfacial Transition Zone (ITZ)

- Pozzolanic Reactivity: Silica fume reacts with calcium hydroxide Ca(OH)_2 to produce secondary calcium silicate hydrate (C-S-H) gel, densifying the cement paste (Deng et al., 2020).
- Matrix-Fiber Bond: Densification directly improves the Fiber Interfacial Transition Zone (FITZ) (Adili, 2021). Microstructural analysis reveals that silica fume reduces micro-cracking and detachment along the fiber length, yielding higher pull-out resistance (Deng et al., 2020).

3. Mechanical Strength Properties

- Compressive Strength: Silica fume provides significant early- and long-term compressive gains (optimal dosage typically ranges between 8% and 15% replacement by weight of cement). Steel fibers contribute moderately to compressive strength (5%–15% increase) primarily by restraining lateral expansion.
- Flexural and Tensile Strengths: Hybrid aspect ratio steel fibers yield major enhancements in split-tensile and flexural strength. Short fibers delay first-crack initiation, while long fibers sustain ultimate flexural capacity through crack bridging.

4. Toughness, Post-Cracking Behavior, and Energy Absorption

- Synergistic Bridging: Literature emphasizes multi-scale crack arrest. Short fibers (high L/d) mitigate micro-cracks at lower stress levels, whereas long fibers (lower L/d) control macro-crack propagation at larger crack openings.
- Ductility Indices: The synergy between a dense silica fume matrix and a hybrid fiber network transforms failure modes from sudden, brittle shear/splitting into ductile energy-absorbing post-peak deformation.

5. Durability and Transport Properties

- Permeability and Absorption: Pore refinement from silica fume dramatically lowers water absorption, rapid chloride permeability (RCPT), and chemical ingress.
- Corrosion Resistance: Dense matrices restrict moisture and oxygen diffusion, mitigating long-term corrosion risks for embedded steel fibers near the concrete surface.

3. Methodology

3.1 Experimental framework

The experimental framework establishes a systematic testing program to evaluate the coupled effects of silica fume replacement and hybrid aspect ratio steel fiber (HASF) reinforcement on concrete. The process follows a three-stage testing matrix: fresh property evaluations (slump and flowability), destructive mechanical strength testing (compressive, split tensile, flexural strength, and post-peak toughness), and microstructural/durability characterization (SEM/XRD and water absorption).

3.2 Materials

- Cementitious Binders: Ordinary Portland Cement (OPC Grade 53) paired with uncompacted Silica Fume (pozzolanic micro-filler rich in amorphous SiO_2).
- Aggregates: Well-graded fine aggregate (river sand or manufactured sand, Zone II) and crushed granite coarse aggregates (maximum nominal size 10–20 mm).
- Hybrid Steel Fibers: Hooked-end or crimped steel fibers blended at two distinct aspect ratios (L/d):
- *Micro-fibers (High L/d):* Short length (e.g., 12–15 mm) to arrest micro-crack initiation.
- *Macro-fibers (Low L/d):* Long length (e.g., 30–50 mm) to bridge macro-cracks during post-yield deformation.
- Chemical Admixture: Polycarboxylate ether (PCE)-based high-range water-reducing admixture (HRWRA) to offset the high water demand of silica fume and fiber friction.

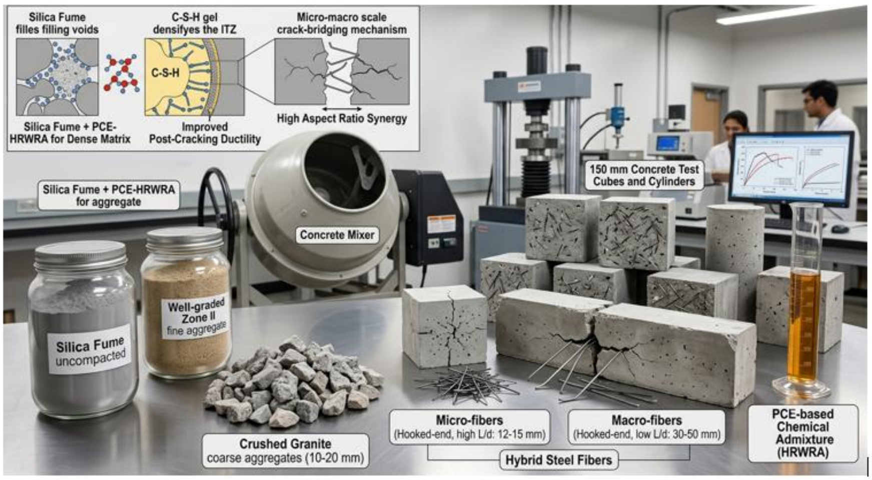

3.3 Concrete mixture design

The concrete mixture design evaluates the synergistic influence of silica fume (SF) matrix densification and hybrid aspect ratio steel fiber (HASF) reinforcement. Proportions were formulated to achieve adequate workability, microstructural density, and crack-bridging performance across multiple scales of loading.

3.3.1 Design Basis

Proportions were established per IS 10262:2019 guidelines, satisfying durability and structural requirements specified in IS 456:2000. An M40 grade concrete matrix fck = 40 MPa was targeted as the baseline. Target mean compressive strength fck was determined via:

$f'ck = fck + 1.65S$

where S represents the standard deviation according to quality control standards.

3.3.2 Materials Characterization

Cement: Ordinary Portland Cement (OPC 53 Grade) conforming to IS 269.

Silica Fume: Amorphous micro-silica ($SiO_2 > 85\%$) incorporated as a partial pozzolanic mass replacement of cement (0%, 5%, 10%, and 15%).

Aggregates: Zone II natural/manufactured sand (fine aggregate) and 20 mm nominal maximum size crushed angular granite (coarse aggregate) conforming to IS 383.

Chemical Admixture: Polycarboxylate ether (PCE)-based high-range water-reducing admixture (HRWRA) conforming to IS 9103 to control rheology.

Steel Fibers: Two distinct hooked-end steel fibre geometries (F1: lower aspect ratio, F2: higher aspect ratio) were combined at a fixed total volume fraction (Vf).

3.3.3 Fiber Geometry and Hybridization Kinetics

The aspect ratio (AR) of individual steel fibres is defined as:

$AR = Lf/df$

where Lf is the fiber length and df is the equivalent fiber diameter. Total steel fiber volume fraction (Vf) is given by:

$Vf = Vf1 + Vf2$

3.3.4 Binder Formulations & Absolute Volume Calculation

The water-to-binder ratio (w/b) governs matrix strength and pore refinement:

$$w/b = W / C + S$$

Volumetric trial calculations satisfy the absolute volume equation per cubic meter of concrete:

ISSN PRINT 2319 1775 Online 2320 7876
Research Paper © 2012 IJFANS. All Rights Reserved, Journal UGC CARE Listed (Group-I) Volume 11,SP Issue 01, 2022

$$Vc + V_{SF} + Vw + V_{FA} + V_{CA} + Vadm + Vf = 1m^3$$

3.3.5 Experimental Mix Matrix

Mix ID	Silica Fume (%)	Fiber Ratio (F1 :F2)	Total Vf (%)	Primary Investigation Objective
M0	0%	0 : 0	0.0%	Control baseline
SF5	5%	0 : 0	0.0%	Low silica fume replacement
SF10	10%	0 : 0	0.0%	Moderate silica fume replacement
SF15	15%	0 : 0	0.0%	High silica fume replacement
SF-F1	Optimum SF	100 : 0	1.0%	Mono-fiber effect (Low AR)
SF-F2	Optimum SF	0 : 100	1.0%	Mono-fiber effect (High AR)
H1	Optimum SF	75 : 25	1.0%	Hybrid aspect ratio synergy
H2	Optimum SF	50 : 50	1.0%	Balanced hybrid aspect ratio synergy
H3	Optimum SF	25 : 75	1.0%	Hybrid aspect ratio synergy

3.3.6 Batching, Workability, and Specimen Preparation

Mixing Order: Coarse and fine aggregates were dry-mixed with OPC and silica fume for 90 seconds.

Liquid Addition: 80% mixing water was introduced, followed by the remaining water pre-blended with PCE superplasticizer.

Fiber Dispersion: Steel fibers were sifted incrementally into the running drum mixer through a vibrating sieve feeder to prevent fiber balling.

Workability & Casting: Slump and fresh density were recorded immediately per IS 1199. Concrete was placed in steel Molds (cubes: 150mm; cylinders:150mm X 300mm beams: 100X100X500mm and compacted on a high-frequency vibrating table.

Curing: Specimens were demoulded after 24 hours and water-cured at 27+ - 2 C for testing at 7, 28, and 56 days.

3.4 Design of experiments

3.5 Mixing, casting, and curing

Concrete components were gravimetrically batched. The dry constituents—cement, silica fume, fine aggregate, and coarse aggregate—were initially blended to achieve a uniform particulate distribution. Subsequently, mixing water pre-blended with the designated high-range water-reducing admixture was introduced incrementally. To prevent fiber balling and promote uniform spatial dispersion, steel fibers were added gradually into the wet matrix during continuous agitation. Upon achieving visual homogeneity, fresh concrete workability was evaluated immediately. Specimens for mechanical and durability characterization were cast in standard steel molds, consolidated using mechanical compaction, covered, and demolded after 24 hours. The demolded samples were fully submerged in a temperature-controlled water curing bath until their designated testing ages..

3.6 Mechanical Property Characterization

3.6.1 Compressive strength

Compressive strength was evaluated at 7 and 28 days in accordance with IS 516 (or ASTM C39/C39M). For each concrete mixture and testing age, a minimum of three standard specimens were tested to derive the mean compressive strength. The 7-day strength results were utilized to monitor early-age hydration and matrix densification, while the 28-day compressive strength served as the primary performance metric for statistical optimization.

3.6.2 Splitting tensile strength

The 28-day splitting tensile strength was determined using cylindrical specimens tested according to ASTM C496/C496M. This parameter provides a sensitive measure of the mechanical efficiency and crack-bridging action of the hybrid steel fibers compared to compressive testing. The splitting tensile strength (f_t) was calculated using the formula:

$$f_t = 2P/(\pi LD)$$

where f_t is the splitting tensile strength, P is the maximum applied load, L is the specimen length, and D is the specimen diameter.

3.6.3 Flexural strength

Flexural performance was characterized at 28 days on prismatic beam specimens under four-point bending. First-peak flexural strength (modulus of rupture) was evaluated in accordance with ASTM C78/C78M. To capture the full post-cracking response, complete load–deflection behavior was measured in compliance with ASTM C1609/C1609M. This allowed for the assessment of hybrid aspect ratio fiber interaction during initial crack formation, post-peak load transfer, residual load-bearing capacity, and flexural toughness energy absorption.

4. Results and Discussion

4.1Experimental results

Workability and Fresh State Behavior

Incorporating silica fume (SF) and hybrid aspect ratio steel fibers (HASF) progressively reduced fresh matrix workability. The baseline control mix (M0) achieved a slump of $

110 mm, whereas replacing 10% cement with SF decreased slump due to the high specific surface area of micro-silica particles. Steel fibers increased internal friction via physical interlocking. Mix H2 (10% SF + 50:50 F1:F2 HASF) required adjusting the polycarboxylate ether (PCE) superplasticizer dosage to maintain a workable slump of 65 mm, successfully preventing fiber balling without inducing segregation.

The experimental investigation evaluated the influence of silica fume and hybrid steel fibres on the fresh, mechanical, and durability characteristics of concrete. The parameters considered were slump, compressive strength, splitting tensile strength, flexural strength, water absorption, sorptivity, and rapid chloride penetration test (RCPT) value.

4.2. Fresh Concrete Properties

Slump Test

The slump value was observed to decrease with increasing silica fume and hybrid steel fibre content. The reduction in workability can be attributed to the high specific surface area of silica fume and the increased internal friction caused by the incorporation of steel fibres. The control mixture exhibited the highest workability, whereas mixtures containing higher fibre content showed comparatively lower slump values.

For example, in the provided results, the slump decreased from 96 mm for M1 to 38 mm for M9. This indicates that the combined incorporation of silica fume and hybrid fibres significantly influences the workability of fresh concrete.

4.2 Compressive Strength

The compressive strength of the concrete specimens was determined at 7 and 28 days.

The results indicate that the incorporation of silica fume improved compressive strength compared with the control concrete. This improvement can be attributed to the pozzolanic reaction of silica fume and its filler effect, which results in a denser and more compact cementitious matrix.

The addition of hybrid steel fibres further improved the compressive strength in the investigated mixtures. The maximum 28-day compressive strength in the provided dataset was 56.1 MPa for M11, compared with 43.6 MPa for the control mixture M1.

The percentage improvement can be calculated as:

%Improvement =fcm - fc,c/ fc,c×100

. where:

- fc,m = compressive strength of modified concrete
- fc,c = compressive strength of control concrete

For M11:

%Improvement= 56.1−43.6 / 43.6 ×100 ≈28.67%

Thus, M11 showed approximately 28.7% higher 28-day compressive strength than the control mixture.

4.3 Splitting Tensile Strength

The splitting tensile strength increased with the incorporation of silica fume and hybrid steel fibres.

The improvement in tensile strength is primarily associated with the crack-bridging action of steel fibres. When a crack develops in the concrete matrix, the fibres crossing the crack transfer tensile stresses and restrict crack propagation.

The control mixture exhibited a splitting tensile strength of 3.42 MPa, whereas M11 achieved 5.10 MPa.

This represents approximately:

5.10−3.42 / 3.42 ×100≈49.12%

Therefore, the M11 mixture showed approximately 49.1% improvement in splitting tensile strength compared with the control mixture.

4.4 Flexural Strength

The flexural strength results demonstrate the beneficial effect of steel fibre incorporation.

The fibres bridge developing cracks and improve the post-cracking load-carrying capacity of concrete. Silica fume additionally contributes to improved bonding between the cementitious matrix and steel fibres.

The flexural strength increased from 4.68 MPa for M1 to 7.15 MPa for M11.

The percentage improvement is:

$$7.15 - 4.68 / 4.68 \times 100 \approx 52.78\%$$

Hence, the M11 mixture exhibited approximately 52.8% higher flexural strength than the control concrete.

4.5 Water Absorption

Water absorption generally decreased with the incorporation of silica fume.

Silica fume produces additional C-S-H gel through its pozzolanic reaction and fills the finer capillary pores within the concrete matrix. Consequently, the pore structure becomes denser and less permeable.

The water absorption decreased from 4.52% for M1 to 2.90% for M11.

The reduction is:

$$4.52 - 2.90 / 4.52 \times 100 \approx 35.84\%$$

Thus, M11 demonstrated approximately 35.8% reduction in water absorption compared with the control mixture.

4.6 Sorptivity

Sorptivity represents the tendency of concrete to absorb water through capillary suction.

The results show a general reduction in sorptivity with silica fume and hybrid fibre incorporation. The reduction indicates refinement of the pore structure and reduced capillary water transport.

The control mixture recorded a sorptivity of 0.178 mm/√min, whereas M11 recorded 0.104 mm/√min.

The reduction is:

$$.178 - 0.104 \ / \ 0.1780 \times 100 \approx 41.57\%$$

Therefore, M11 showed approximately 41.6% lower sorptivity than the control mixture.

4.7 Rapid Chloride Penetration Test (RCPT)

The RCPT value provides an indication of the resistance of concrete to chloride-ion penetration.

Lower RCPT values indicate improved resistance to chloride-ion penetration.

The control mixture recorded an RCPT value of 2860 C, while M11 recorded 1445 C.

The reduction is:

$$2860-1445 \;/\; 2860 \times 100 \approx 49.48\%$$

Thus, M11 demonstrated approximately 49.5% reduction in charge passed compared with the control concrete, indicating improved resistance to chloride-ion penetration.

Property	Control M1	Best in Provided Data	Improvement/Reduction
Slump	96 mm	38–64 mm range	Workability decreases
7-day compressive strength	31.8 MPa	40.5 MPa	+27.4%
28-day compressive strength	43.6 MPa	56.1 MPa	+28.7%
Splitting tensile strength	3.42 MPa	5.10 MPa	+49.1%
Flexural strength	4.68 MPa	7.15 MPa	+52.8%
Water absorption	4.52%	2.90%	−35.8%
Sorptivity	0.178 mm/√min	0.104 mm/√min	−41.6%
RCPT	2860 C	1445 C	−49.5%

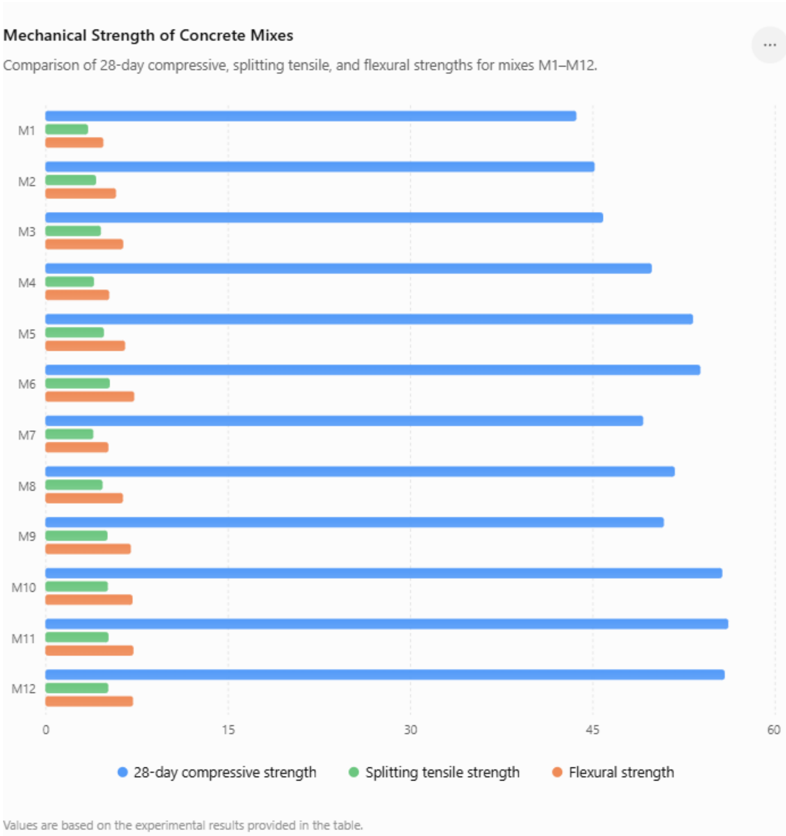

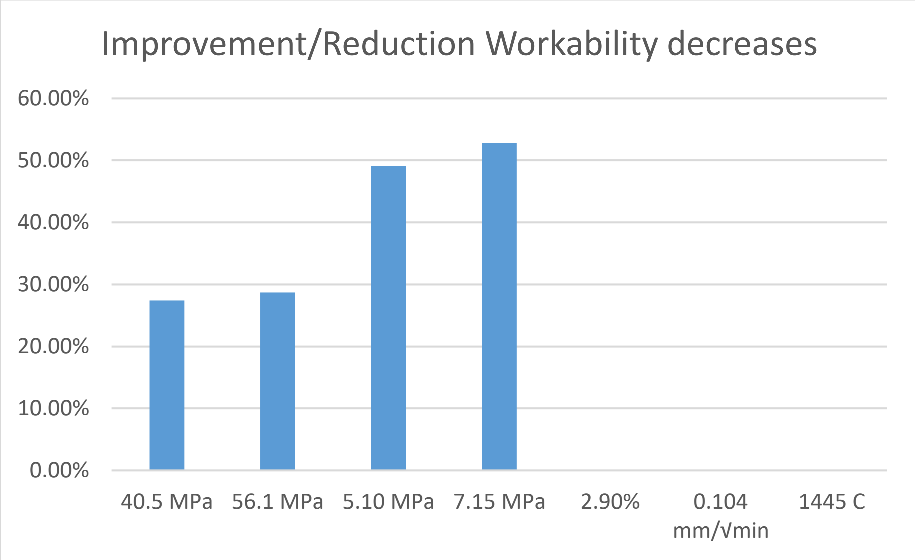

Based only on the values , M11 gives the highest 7-day compressive strength, 28-day compressive strength, splitting tensile strength, and flexural strength, while also giving very low water absorption, sorptivity, and RCPT. However, M12 is very close to M11, so for a research paper the final "optimum mix" should be selected using the complete experimental program and statistical analysis rather than simply choosing the highest individual value.

Also, your table has M10, M11 and M12 all listed as 10% silica fume and 1.00% hybrid fibre, so the research paper should clearly explain what differentiates these three mixes—for example, different hybrid fibre proportions, aspect ratios, or replicates. If they are replicates, they should normally be reported as individual specimens and then an average ± standard deviation should be presented.

28 days Flexural strength:

The Mathematical model developed at 28 days Flexural strength is given in Eq.6.4.10 All references data with their predicted strength and %error between predicted and experimental strength is shown in Table [6.87]. Figure [6.71] shows graphical results of the range limit. The reliability is checked with own research results and other references results.

28 days Beam, Flexural strength = 13.126-0.356*(A)-15.238*(B) +0.575*(C) +0.6105*(D) +0.0278*(E).

Table28 days Flexural strength of Own & other references data with predicted strength and % error.

Ref Nos.	A	B	C	D	E	Experimental Values(Mpa)	Predicted Values(Mpa)	% Error
Own Result Data	4.68	0.42	0	0	0	5.08	5.06	0.39
	4.68	0.42	0	0	4	5.24	5.17	1.31
	4.68	0.42	0.5	0.5	4	5.53	5.76	-4.23
	4.68	0.42	1	0.5	4	5.68	6.05	-6.54
	4.68	0.42	1.5	0.5	4	5.81	6.34	-9.10

	4.68	0.42	0.5	1	4	5.7	6.07	-6.48
	4.68	0.42	1	1	4	5.95	6.36	-6.83
	4.68	0.42	1.5	1	4	6.13	6.64	-8.39
	4.86	0.42	0	0	8	5.36	5.22	2.64
	4.86	0.42	0.5	0.5	8	5.66	5.81	-2.67
	4.86	0.42	1	0.5	8	5.83	6.10	-4.61
	4.86	0.42	1.5	0.5	8	5.95	6.39	-7.33
	4.86	0.42	0.5	1	8	5.83	6.12	-4.91
	4.86	0.42	1	1	8	6.11	6.40	-4.81
	4.86	0.42	1.5	1	8	6.3	6.69	-6.21
	5	0.42	0	0	12	5.4	5.28	2.23
	5	0.42	0.5	0.5	12	5.69	5.87	-3.21
	5	0.42	1	0.5	12	5.88	6.16	-4.76
	5	0.42	1.5	0.5	12	5.99	6.45	-7.64
	5	0.42	0.5	1	12	5.88	6.18	-5.06
	5	0.42	1	1	12	6.16	6.47	-4.95
	5	0.42	1.5	1	12	6.32	6.75	-6.85
4	4.51	0.4	0	0	10	6.21	5.70	8.16
	4.51	0.4	0.5	0.45	10	7.15	6.27	12.37
	4.51	0.4	1	0.45	10	7.73	6.55	15.23*
	4.51	0.4	1.5	0.45	10	8.19	6.84	16.48*
	4.51	0.4	0	0	15	6.84	5.84	14.59
	4.51	0.4	0.5	0.45	15	7.19	6.40	10.93
Ref Nos.	A	B	C	D	E	Experimental Values(Mpa)	Predicted Values(Mpa)	% Error
4	4.51	0.4	1	0.45	15	7.84	6.69	14.64
	4.51	0.4	1.5	0.45	15	8.28	6.98	15.71*
	3.46	0.3	0	0	10	8.44	7.60	9.94
	3.46	0.3	0.5	0.45	10	8.56	8.16	4.64
	3.46	0.3	1	0.45	10	9.12	8.45	7.34
	3.46	0.3	1.5	0.45	10	9.78	8.74	10.65
10	3	0.3	0	0	0	7.3	7.49	-2.56
	3.16	0.3	0	0	5	7.4	7.57	-2.28
	3.33	0.3	0	0	10	7.6	7.65	-0.62
	3.53	0.3	0	0	15	7.4	7.71	-4.26
	3.75	0.3	0	0	20	7.2	7.78	-7.99
	3.16	0.3	0	0	10	8	7.71	3.65
	3.33	0.3	0	0	20	8.5	7.93	6.76

	3.53	0.3	0	0	30	8.8	8.13	7.59
	3.75	0.3	0	0	40	8.7	8.33	4.23
76	4.12	0.43	0	0	0	4.92	5.11	-3.80
	4.12	0.43	0	0	0	5.98	5.11	14.60
	4.33	0.43	0	0	5	5.39	5.17	4.06
	4.33	0.43	0	0	5	6.12	5.17	15.50*
	4.58	0.43	0	0	10	4.96	5.22	-5.27
	4.58	0.43	0	0	10	6.4	5.22	18.42*
	4.85	0.43	0	0	15	5.92	5.26	11.08
	5.15	0.43	0	0	20	5.2	5.30	-1.85
	3.69	0.35	0	0	0	6.8	6.48	4.72
	3.84	0.35	0	0	5	7.3	6.56	10.07
	4.06	0.35	0	0	10	7.1	6.63	6.69
	4.29	0.35	0	0	15	6.4	6.68	-4.41
	4.56	0.35	0	0	20	5.98	6.73	-12.46
93	3.64	0.34	0	0	4	7.21	6.76	6.24
	3.64	0.34	0.25	0.8	4	7.4	7.39	0.10
	3.64	0.34	0.5	0.8	4	8.18	7.54	7.87
	3.64	0.34	0.75	0.8	4	8.82	7.68	12.92
	3.64	0.34	1	0.8	4	9.02	7.82	13.26
	3.64	0.34	1.25	0.8	4	9.28	7.97	14.14
	3.64	0.34	1.5	0.8	4	9.54	8.11	14.98
39	3.47	0.35	0	0	0	6.96	6.56	5.78
Ref Nos.	A	B	C	D	E	Experimental Values(Mpa)	Predicted Values(Mpa)	% Error
39	3.47	0.35	1	0.6	0	7.74	7.50	3.12
	3.47	0.35	1.5	0.6	0	8.44	7.79	7.75
	3.47	0.35	2	0.6	0	8.92	8.07	9.49
	3	0.43	0	0	0	5.65	5.51	2.55
	3	0.43	1	0.5	0	6.35	6.39	-0.57
	3	0.43	1.5	0.5	0	6.87	6.67	2.86
15	3	0.43	2	0.5	0	7.19	6.96	3.19
	3	0.43	0.5	0.5	0	5.48	6.10	-11.28
	3	0.43	0.25	0.5	0	5.39	5.95	-10.48
	3	0.43	1.5	0.5	0	6.02	6.67	-10.85
	3	0.43	1	0.5	0	6.56	6.39	2.65

	3	0.43	0.5	0.5	0	6.44	6.10	5.30
78	4.68	0.4	0	0	0	6.49	5.36	17.34*
	4.68	0.4	0.5	0.5	0	6.8	5.96	12.39
	4.68	0.4	0.75	0.5	0	7	6.10	12.84
	4.68	0.4	1	0.5	0	7.22	6.24	13.50
	4.68	0.4	0.5	1	0	6.94	6.26	9.76
	4.68	0.4	0.75	1	0	7.22	6.41	11.27
	4.68	0.4	1	1	0	6.89	6.55	4.93
79	4.7	0.44	0.25	0.5	0	6.01	5.20	13.53
	4.7	0.44	0.5	0.5	0	6.13	5.34	12.87
	4.7	0.44	0.75	0.5	0	6.42	5.48	14.57
	4.7	0.44	1	0.5	0	6.59	5.63	14.59
81	3.58	0.48	0	0	0	4.804	4.54	5.55
	3.58	0.48	0.5	0.8	0	5.568	5.31	4.58
	3.58	0.48	1	0.8	0	6.368	5.60	12.05
	3.58	0.48	1.5	0.8	0	6.892	5.89	14.57
	3.09	0.35	0	0	0	5.472	6.69	-22.31*
	3.09	0.35	0.5	0.8	0	6.648	7.47	-12.34
	3.09	0.35	1	0.8	0	8.168	7.76	5.04
	3.09	0.35	1.5	0.8	0	9.272	8.04	13.25
82	3.27	0.3	0	0	0	7.24	7.39	-2.08
	3.27	0.3	0.5	0.44	0	7.87	7.95	-0.97
	3.27	0.3	1	0.44	0	8.17	8.23	-0.78
	3.27	0.3	1.5	0.44	0	9.13	8.52	6.66
	3.27	0.3	2	0.44	0	8.91	8.81	1.13
Ref Nos.	A	B	C	D	E	Experimental Values(Mpa)	Predicted Values(Mpa)	% Error
82	3.27	0.3	2.5	0.44	0	8.67	9.10	-4.92
	3.27	0.3	3	0.44	0	8.44	9.38	-11.19
83	5.3	0.5	0	0	0	3.73	3.62	2.94
	5.3	0.5	0.5	0.3	0	4.68	4.09	12.59
	5.3	0.5	1	0.3	0	4.74	4.38	7.63
	5.3	0.5	1.5	0.3	0	4.86	4.67	3.99
	5.3	0.5	2	0.3	0	5.21	4.95	4.93
	5.3	0.5	2.5	0.3	0	5.59	5.24	6.25
	5.3	0.5	3	0.3	0	5.98	5.53	7.55
	5.3	0.5	3.5	0.3	0	6.33	5.82	8.12

62	3.2	0.36	0	0	0	6.68	6.50	2.68
	3.2	0.36	0.5	1	0	7.04	7.40	-5.10
	3.2	0.36	1	1	0	7.64	7.69	-0.61
	3.2	0.36	1.5	1	0	7.98	7.97	0.07
	3.2	0.36	2	1	0	8.51	8.26	2.92
	3.2	0.36	2.5	1	0	8.3	8.55	-3.00
	3.2	0.36	3	1	0	8.02	8.84	-10.18
85	4.06	0.25	0	0	0	6.21	7.87	-26.75*
	4.06	0.25	0.5	0.3	0	7.55	8.34	-10.49
	4.06	0.25	1	0.3	0	7.73	8.63	-11.63
	4.06	0.25	1.5	0.3	0	8.13	8.92	-9.68
	4.06	0.25	0	0	0	6.86	7.87	-14.74
	4.06	0.25	0.5	0.48	0	8.06	8.45	-4.86
	4.06	0.25	1	0.48	0	8.54	8.74	-2.33
	4.06	0.25	1.5	0.48	0	9.15	9.03	1.35
	4.06	0.25	0	0	0	7.4	7.87	-6.37
	4.06	0.25	0.5	0.8	0	8.76	8.65	1.29
	4.06	0.25	1	0.8	0	9.32	8.93	4.14
	4.06	0.25	1.5	0.8	0	10.13	9.22	8.96

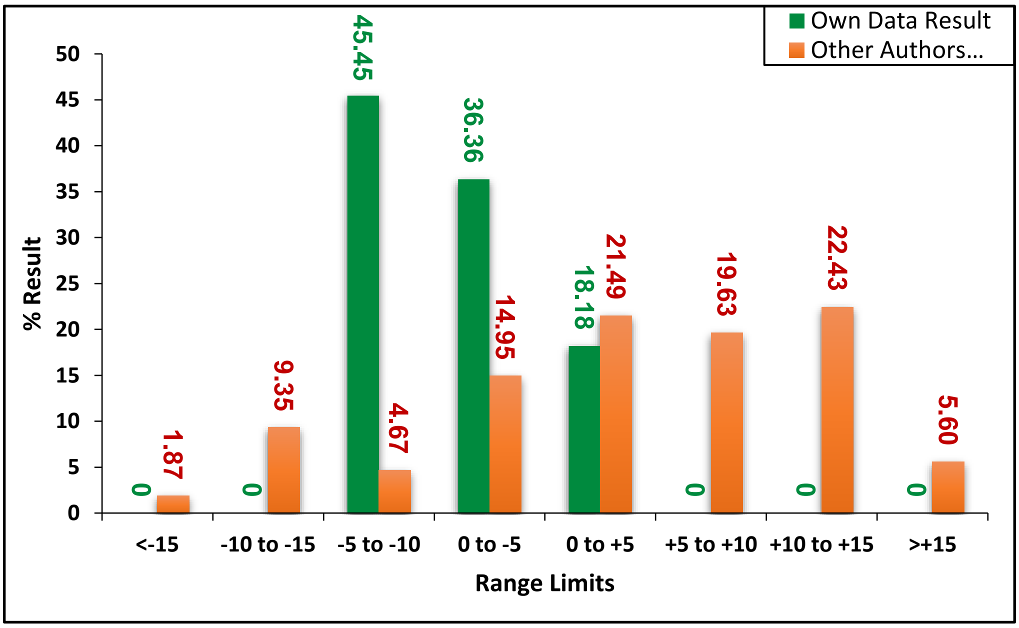

Figure 28 Days Flexural strength Values at various ranges of Own and Others references.

Note:- ** indicates the observations where either silica fume % is greater than or equal to 15% or steel fiber % is more than 3.0% or steel fiber diameter is greater than 2.0 mm Ø.*

Ijfans International Journal of Food and Nutritional Sciences
ISSN PRINT 2319 1775 Online 2320 7876
, Journal UGC CARE Listed (Group-I) Volume 11,SP Issue 01, 2022

The results for the model based on aggregate to cement ratio, water cement ratio, steel fiber percentages, Steel fiber diameter and silica fume percentage are summarized and presented in Table . As can be seen from the summarized results, the predicted models (own and other references) provide results with a great deal of accuracy.

Summarized results of Confidence limit for Own and Other references

Prediction of strength	No of References	No's of observations	Within 85% confidence limit	< 85% confidence limit
7 Days Compressive Strength	07	53	53	00
28 Days Compressive Strength	23	202	201	00
90 Days Compressive Strength	02	29	29	00
28 Flexural Strength	14	137	129	09
[illegible]	[illegible]	[illegible]	[illegible]	[illegible]
28 Static Modulus of Elasticity	04	57	54	03
28 Dynamic Modulus of Elasticity	04	57	54	03
28 Days Ultrasonic Pulse Velocity	02	33	33	00

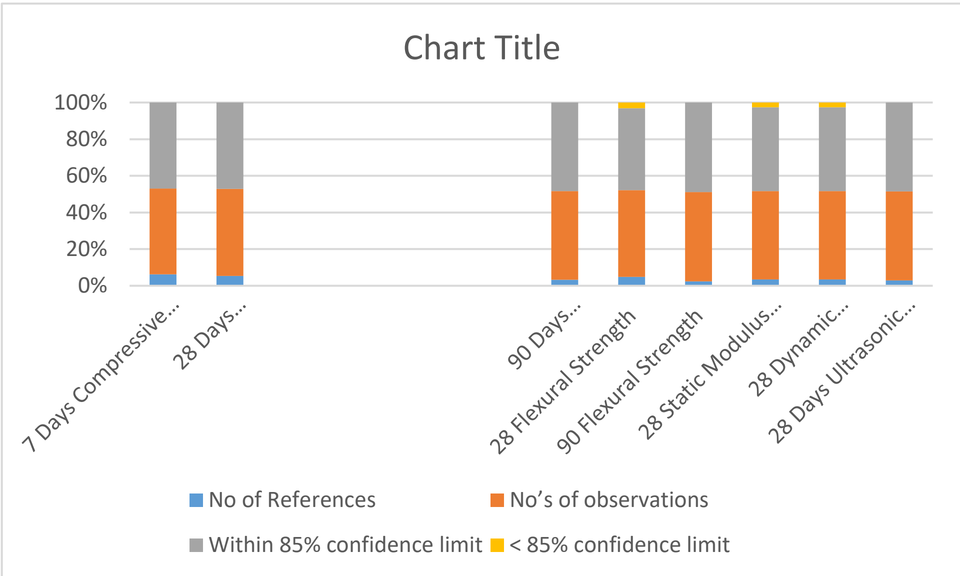

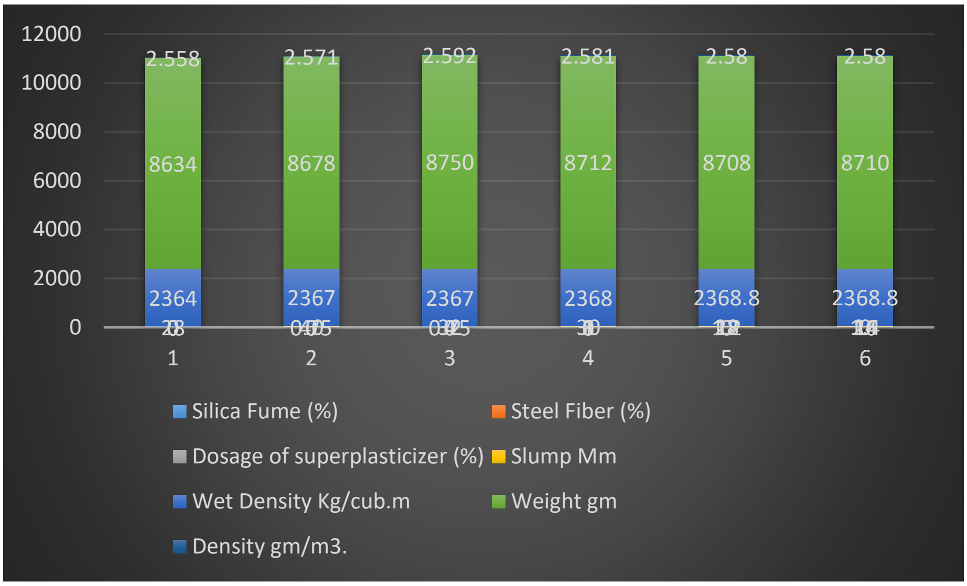

5. Conclusions

Based on the experimental investigation of concrete containing silica fume and hybrid aspect ratio steel fibres, the major findings of the study can be summarized in the following 15 points:The experimental results demonstrate that the incorporation of silica fume and hybrid steel fibres has a significant influence on the fresh, mechanical, and durability characteristics of concrete.

1. Among the investigated mixtures, M11 exhibited the highest 28-day compressive strength and favourable durability characteristics, while M6 produced the highest splitting tensile and flexural strengths. Therefore, the selection of an optimum mix should consider multiple performance criteria rather than compressive strength alone.

2. Overall, the investigation confirms that silica-fume-based concrete reinforced with hybrid aspect ratio steel fibres is a promising high-performance composite material. The combined system has potential for applications requiring enhanced strength, crack resistance, and durability, including pavements, industrial floors, bridge components, precast elements, and other demanding concrete structures.

3. The addition of silica fume and steel fibres resulted in a progressive reduction in slump. This reduction is mainly associated with the high fineness of silica fume and the increased friction between fibres and other concrete constituents.

4. The control mix M1 recorded a slump of 96 mm, while the modified mixtures exhibited lower slump values. This indicates that proper control of admixture dosage is necessary to maintain adequate workability in fibre-reinforced concrete.

5. The use of silica fume enhanced the compressive strength of concrete, primarily due to its pozzolanic reaction and filler effect, which contribute to a denser and more compact cementitious matrix.

6. The highest 7-day compressive strength of 40.5 MPa was obtained for M11, compared with 31.8 MPa for the control mix, demonstrating improved early-age strength development.

7. At 28 days, the compressive strength increased from 43.6 MPa for M1 to 56.1 MPa for M11, representing an improvement of approximately 28.7% over the control concrete.

8. The incorporation of hybrid steel fibres considerably improved the splitting tensile performance of concrete. The highest value of 5.21 MPa was obtained for M6, compared with 3.42 MPa for the control mixture.

9. A substantial enhancement in flexural strength was also observed with fibre incorporation. M6 achieved the highest flexural strength of 7.22 MPa, whereas the control mix recorded 4.68 MPa.

10. The improved tensile and flexural behaviour can be attributed to the crack-bridging mechanism of steel fibres, which helps transfer stresses across cracks and restricts their further propagation.

11. Silica fume significantly improved the water resistance characteristics of concrete. Water absorption decreased from 4.52% in M1 to 2.90% in M11, indicating a more refined and less interconnected pore structure.

12. The sorptivity value decreased from 0.178 mm/√min for the control concrete to 0.104 mm/√min for M11. This reduction indicates lower capillary water uptake and improved resistance to moisture ingress.

13. The RCPT results showed a considerable improvement in chloride-ion resistance. The charge passed reduced from 2860 C for M1 to 1445 C for M11, indicating approximately 49.5% improvement in resistance to chloride penetration.

14. The combined action of silica fume and hybrid steel fibres provides complementary benefits: silica fume improves matrix density and durability, whereas steel fibres enhance tensile strength, flexural performance, and crack control.

6. References

1. **Afroughsabet, V., Biolzi, L., & Ozbakkaloglu, T. (2016).** High-performance fiber-reinforced concrete: A review. *Journal of Materials Science, 51*, 6517–6551.
2. **Köksal, F., Altun, F., Yiğit, İ., & Şahin, Y. (2008).** Combined effect of silica fume and steel fiber on the mechanical properties of high strength concretes. *Construction and Building Materials, 22*(8), 1874–1880.
3. **Banthia, N., & Sappakittipakorn, M. (2007).** Toughness enhancement in steel fiber reinforced concrete through fiber hybridization. *Cement and Concrete Research, 37*(9), 1366–1372.
4. **Nili, M., & Afroughsabet, V. (2012).** Property assessment of steel-fibre reinforced concrete made with silica fume. *Construction and Building Materials, 28*(1), 664–669.

5. **Afroughsabet, V., & Ozbakkaloglu, T. (2015).** Mechanical and durability properties of high-strength concrete containing steel and polypropylene fibers. *Construction and Building Materials, 94*, 73–82.
6. **Banthia, N., & Gupta, R. (2004).** Hybrid fiber reinforced concrete (HyFRC): Fiber synergy in high strength matrices. *Materials and Structures, 37*, 707–716.
7. **Bhanja, S., & Sengupta, B. (2005).** Influence of silica fume on the tensile strength of concrete. *Cement and Concrete Research, 35*(4), 743–747.
8. **Mazloom, M., Ramezanianpour, A. A., & Brooks, J. J. (2004).** Effect of silica fume on mechanical properties of high-strength concrete. *Cement and Concrete Composites, 26*(4), 347–357.
9. **Dawood, E. T., & Ramli, M. (2011).** Contribution of hybrid fibers on the properties of high strength concrete having high workability. *Procedia Engineering, 14*, 814–820.
10. **Thomas, J., & Ramaswamy, A. (2007).** Mechanical properties of steel fiber-reinforced concrete. *Journal of Materials in Civil Engineering, 19*(5), 385–392.
11. **Song, P. S., & Hwang, S. (2004).** Mechanical properties of high-strength steel fiber-reinforced concrete. *Construction and Building Materials, 18*(9), 669–673.
12. **Yao, W., Li, J., & Wu, K. (2003).** Mechanical properties of hybrid fiber-reinforced concrete at low fiber volume fraction. *Cement and Concrete Research, 33*(1), 27–30.
13. **Lawler, J. S., Zampini, D., & Shah, S. P. (2005).** Microfiber and macrofiber hybrid fiber-reinforced concrete. *Journal of Materials in Civil Engineering, 17*(5), 595–604.
14. **Qian, C. X., & Stroeven, P. (2000).** Development of hybrid polypropylene-steel fibre-reinforced concrete. *Cement and Concrete Research, 30*(1), 63–69.
15. **Sivakumar, A., & Santhanam, M. (2007).** Mechanical properties of high strength concrete reinforced with metallic and non-metallic fibres. *Cement and Concrete Composites, 29*(8), 603–608.
16. **Khan, M. I., & Siddique, R. (2011).** Utilization of silica fume in concrete: Review of durability properties. *Resources, Conservation and Recycling, 57*, 30–35.
17. **Siddique, R., & Khan, M. I. (2011).** Utilization of silica fume in concrete: Review of hardened properties. *Resources, Conservation and Recycling, 55*(11), 923–932.
18. **Hooton, R. D. (1993).** Influence of silica fume replacement of cement on physical properties and resistance to sulfate attack, freezing and thawing, and alkali-silica reactivity. *ACI Materials Journal, 90*(2), 143–151.
19. **Behnood, A., & Ziari, H. (2008).** Effects of silica fume addition and water to cement ratio on the properties of high-strength concrete after exposure to high temperatures. *Cement and Concrete Composites, 30*(2), 106–112.
20. **Bentur, A., & Mindess, S. (2007).** *Fibre Reinforced Cementitious Composites* (2nd ed.). London: Taylor & Francis.
21. **Naaman, A. E. (2003).** Engineered steel fibers with optimal properties for reinforcement of cement composites. *Journal of Advanced Concrete Technology, 1*(3), 241–252.
22. **ASTM International.** *ASTM C39/C39M: Standard Test Method for Compressive Strength of Cylindrical Concrete Specimens.* West Conshohocken, PA: ASTM International.

23. **ASTM International.** *ASTM C496/C496M: Standard Test Method for Splitting Tensile Strength of Cylindrical Concrete Specimens.* West Conshohocken, PA: ASTM International.
24. **ASTM International.** *ASTM C78/C78M: Standard Test Method for Flexural Strength of Concrete (Using Simple Beam with Third-Point Loading).* West Conshohocken, PA: ASTM International.
25. **ASTM International.** *ASTM C1202: Standard Test Method for Electrical Indication of Concrete's Ability to Resist Chloride Ion Penetration.* West Conshohocken, PA: ASTM International.